Calculation of thin-walled axisymmetrically loaded structures of the AIC taking into account FEM-based physical nonlinearity

Arsen Dzhabrailov[1,*], *Anatoly* Nikolaev[1], and *Natalya* Gureeva[2]

[1]Volgograd State Agrarian University, 400002 Volgograd, Russia
[2] Financial University under the Government of the Russian Federation, 125167 Moscow, Russia

Abstract. The article describes an algorithm for calculating an axisymmetrically loaded shell structure with a branching meridian, taking into account elastic-plastic deformations when loading based on the deformation theory of plasticity without assuming that the material is incompressible during plastic deformations. The correct relations which determine the static conjugation conditions of several revolution shells in the joint assembly are used. A comparative analysis of finite element solutions is presented for various options plasticity matrix development at the loading stage.

1 Introduction

The theory of thin shells is widely used [1–6]. Due to difficulties in obtaining analytical solutions based on the theory of shells for the designed thin-walled elements, numerical methods have become widespread [7–10]. The action of external loads in the presence of shell meridian branching can cause plastic deformations. Taking into account the nonlinear work of the material, one can evaluate the work of the structure which can develop more economical solutions [11, 12]. When determining the relationships between stress and strain increments based on the deformation theory of plasticity, we used the functional dependence between the average stress and average strain obtained from the tension experiments.

2 Materials and methods

2.1 Shell geometry

The position of arbitrary point M^0 of the middle surface of the axisymmetrically loaded shell of revolution is determined by the radius vector

$$\mathbf{R}^o = x\mathbf{i} + r\mathbf{k}, \quad (1)$$

where x *is* the axis coordinate; r the revolution radius, being function of x;**i** and **k** – unit vectors of the Cartesian coordinate system.

By differentiating (1) with respect to the meridional coordinate s, we can determine the unit vector tangent to the meridian of the shell at arbitrary point M^0 of the middle surface

$$\mathbf{e}_1^0 = \mathbf{R}_{,s}^0 = (\mathbf{i} + r_{,x}\mathbf{k})x_{,s}. \quad (2)$$

The unit vector of the normal to the shell surface at arbitrary point M^0 is determined by the vector product

$$\mathbf{e}^0 = \mathbf{e}_1^0 \times \mathbf{j} = -r_{,x}\, x_s \mathbf{i} + x_s \mathbf{k}. \quad (3)$$

Equalities (2) and (3) are presented in the matrix

$$\{\mathbf{e}^o\} = [m^o]\{\mathbf{i}\}, \quad (4)$$

where $\{\mathbf{e}^o\}^T = \{\mathbf{e}_1^0 \mathbf{e}^0\}$; $\{\mathbf{i}\} = \{\mathbf{ik}\}$.

Derivatives of local basis vectors are determined by expressions

$$\mathbf{e}_{1,s}^0 = x_{,ss}\,\mathbf{i} + (r_{,xx}\,x_{,s}^2 + r_{,x}\,x_{,ss})\mathbf{k};$$
$$\mathbf{e}_{,s}^0 = -(r_{,xx}\,x_{,s}^2 + r_{,x}\,x_{,ss})\mathbf{i} + x_{,ss}\,\mathbf{k}. \quad (5)$$

In the matrix form of expression (5) they are as follows

$$\{\mathbf{e}_{,s}^0\} = [m]\{\mathbf{i}\}, \quad (6)$$

where $\{\mathbf{e}_{,s}^0\} = \{\mathbf{e}_{1,s}^0 \mathbf{e}_{,s}^0\}$.

From (4) we can obtain the matrix dependence

$$\{\mathbf{i}\} = [m^o]^{-1}\{\mathbf{e}^o\}. \quad (7)$$

Given (7) expression (6) is written as follows

$$\{\mathbf{e}_{,s}^0\} = [m][m^o]^{-1}\{\mathbf{e}^o\} = [n]\{\mathbf{e}^o\}. \quad (8)$$

In the process of shell deformation, the point of its middle surface is considered in three positions: initial (point M^0), after loading steps j (point M, displacement vector v), and after the (j + 1)-th loading step (M*, displacement vector Δ**v**). At a distance ζ from the middle surface, the following points$M^{0\zeta}$,M^{ζ}и$M^{*\zeta}$ correspond to it. When taking into account the hypothesis of direct normals, the position of these points is determined by the following radius vectors

$$\mathbf{R}=\mathbf{R}^0+\mathbf{v};\ \mathbf{R}^*=\mathbf{R}+\Delta\mathbf{v};\ \mathbf{R}^{0\zeta}=\mathbf{R}^0+\zeta\mathbf{e}^0; \quad (9)$$
$$\mathbf{R}^{\zeta}=\mathbf{R}^{0\zeta}+\mathbf{v}+\zeta(\mathbf{e}_n-\mathbf{e}^0);\ \mathbf{R}^{*\zeta}=\mathbf{R}^{\zeta}+\Delta\mathbf{v}+\zeta(\mathbf{e}_n^*-\mathbf{e}).$$

Displacement vectors **v**and Δ**v,** included in (9), for the FE under study are presented in the basis of point M^0

$$\mathbf{v}=\upsilon^1\mathbf{e}_1^0+\upsilon\mathbf{e}^0; \quad (10)$$
$$\Delta\mathbf{v}=\Delta\upsilon^1\mathbf{e}_1^0+\Delta\upsilon\mathbf{e}^0.$$

By differentiating (10) along the curvilinear coordinate s with allowance for (5), we have

$$\mathbf{v}_{,s}=f_1^1\mathbf{e}_1^0+f_1\mathbf{e}^0;\ \mathbf{v}_{,ss}=f_{11}^1\mathbf{e}_1^0+f_{11}\mathbf{e}^0; \quad (11)$$
$$\Delta\mathbf{v}_{,s}=l_1^1\mathbf{e}_1^0+l_1\mathbf{e}^0;\ \Delta\mathbf{v}_{,ss}=l_{11}^1\mathbf{e}_1^0+l_{11}\mathbf{e}^0.$$

where $f_1^1 \ldots . l_{11}$ are functions of vectors **v**, Δ**v** and coefficients of matrix $[n]$, included in (8).

*Corresponding author: arsen82@yandex.ru

Differentiation (9) determines the basis vectors of an arbitrary point of the shell in a deformed state

$$\mathbf{e}_1^{\zeta} = \mathbf{R}_{,s}^{\zeta} = \mathbf{e}_1^{0\zeta} + \mathbf{v}_{,s} + \zeta\left(\mathbf{e}_{n,s} - \mathbf{e}_{,s}^{0}\right); \quad (12)$$
$$\mathbf{e}_1^{*\zeta} = \mathbf{R}_{,s}^{*\zeta} = \mathbf{e}_1^{\zeta} + \Delta\mathbf{v}_{,s} + \zeta\left(\mathbf{e}_{n,s}^{*} - \mathbf{e}_{,s}\right);$$
$$\mathbf{e}_1^{0\zeta} = \mathbf{R}_{,s}^{0\zeta}; \mathbf{e}_1^{\zeta} = \mathbf{R}_{,s}^{\zeta}.$$

The unit vectors of the normals in the deformed state are expressed by the vector product

$$\mathbf{e}_n = \mathbf{e}_1 \times \mathbf{j} = (\mathbf{R}^0+\mathbf{v})_{,s}\times \mathbf{j} = \left(\mathbf{e}_1^0 + \mathbf{v}_{,s}\right)\times \mathbf{j}; \quad (13)$$
$$\mathbf{e}_n^{*} = \mathbf{e}_1^{*\zeta}\times \mathbf{j} = (\mathbf{R}+\Delta\mathbf{v})_{,s}\times \mathbf{j} = \left(\mathbf{e}_1 + \Delta\mathbf{v}_{,s}\right)\times \mathbf{j}$$

Deformations and their increments in an arbitrary layer of the shell spaced at a distance ζ from the middle surface can be determined on the basis of equations of continuum mechanics [13]

$$\varepsilon_{11}^{\zeta} = \frac{\left(e_{11}^{\zeta} - e_{11}^{0\zeta}\right)}{2}; \ \Delta\varepsilon_{11}^{\zeta} = \frac{\left(e_{11}^{*\zeta} - e_{11}^{\zeta}\right)}{2}; \quad (14)$$
$$\varepsilon_{22}^{\zeta} = \frac{\mathbf{R}^{\boldsymbol{\zeta}}\cdot\mathbf{k} - \mathbf{R}^{\mathbf{0}\boldsymbol{\zeta}}\cdot\mathbf{k}}{\mathbf{R}^{\mathbf{0}\boldsymbol{\zeta}}\cdot\mathbf{k}}; \ \Delta\varepsilon_{22}^{\zeta} = \frac{\mathbf{R}^{*\boldsymbol{\zeta}}\cdot\mathbf{k} - \mathbf{R}^{\boldsymbol{\zeta}}\cdot\mathbf{k}}{\mathbf{R}^{\boldsymbol{\zeta}}\cdot\mathbf{k}}.$$

The covariant components of metric tensors included in (14) in the initial and deformed states are determined by the corresponding scalar products

$$e_{11}^{\zeta} = \mathbf{e}_1^{\zeta}\cdot\mathbf{e}_1^{\zeta}; \quad e_{11}^{0\zeta} = \mathbf{e}_1^{0\zeta}\cdot\mathbf{e}_1^{0\zeta}; \quad (15)$$
$$e_{11}^{*\zeta} = \mathbf{e}_1^{*\zeta}\cdot\mathbf{e}_1^{*\zeta}.$$

As a result, deformations and curvatures of the arbitrary point of the shell of revolution included in (14) for j loading steps are expressed by components of the displacement vector and their derivatives

$$\varepsilon_{11}^{\zeta} = \upsilon_{,s}^{1} - k\upsilon + \zeta\left(-k\upsilon_{,s}^{1} - k_{,s}\,\upsilon^{1} - \upsilon_{,ss}\right); \quad (16)$$
$$\varepsilon_{22}^{\zeta} = \upsilon k_2 + k_1\upsilon^{1} + \zeta(-k_1\upsilon_{,s} - kk_1\upsilon^{1}),$$

where $= r_{,xx}x_{,s}^{3}$, $k_1 = r_{,x}x_{,s}/r$, $k_2 = x_{,s}/r$.

Similarly, for step (j + 1) in a geometrically linear formulan

$$\Delta\varepsilon_{11}^{\zeta} = \Delta\upsilon_{,s}^{1} - k\Delta\upsilon + \zeta\left(-k\Delta\upsilon_{,s}^{1} - k_{,s}\,\Delta\upsilon^{1} - \Delta\upsilon_{,ss}\right); \quad (17)$$
$$\Delta\varepsilon_{22}^{\zeta} = \Delta\upsilon k_2 + k_1\Delta\upsilon^{1} + \zeta(-k_1\Delta\upsilon_{,s} - kk_1\Delta\upsilon^{1}).$$

(16) and (17) can be written as

$$\varepsilon_{\alpha\beta}^{\zeta} = \varepsilon_{\alpha\beta} + \zeta\chi_{\alpha\beta}; \ \Delta\varepsilon_{\alpha\beta}^{\zeta} = \Delta\varepsilon_{\alpha\beta} + \zeta\Delta\chi_{\alpha\beta}. \quad (18)$$

Deformations and curvatures of the point of the middle surface and their increments at the loading stage included in (18) are expressed by matrix ratios

$$\{\varepsilon^{\zeta}\} = [\Gamma]\{\varepsilon\} = [\Gamma][\mathrm{L}]\{\upsilon\},$$
$$\{\Delta\varepsilon^{\zeta}\} = [\Gamma]\{\Delta\varepsilon^{\zeta}\} = [\Gamma][\mathrm{L}]\{\Delta\upsilon\}, \quad (19)$$

where$\{\varepsilon\}^{\mathrm{T}} = \{\varepsilon_{11}\varepsilon_{22}\chi_{11}\chi_{22}\}$;$\{\upsilon\}^{\mathrm{T}} = \{\upsilon^{1}\upsilon\}$;$\{\Delta\varepsilon\}^{\mathrm{T}} = \{\Delta\varepsilon_{11}\Delta\varepsilon_{22}\Delta\chi_{11}\Delta\chi_{22}\}$;$\{\Delta\upsilon\}^{\mathrm{T}} = \{\Delta\upsilon^{1}\Delta\upsilon\}$;[L]-matrix of differential and algebraic operators.

2.2 The final element at the loading stage

Under the axisymmetric loading, the use of a one-dimensional finite element is most effective. A fragment of the shell, bounded by two parallel planes perpendicular to the axis of rotation is displayed on the linear element with coordinates of the nodes $\eta = -1$ and $\eta = 1$, where $\eta -$ the local coordinate used for the numerical integration (Fig. 1).

The meridional (s) and axial (x) coordinates of the shell were considered as functions of the local coordinate η

$$s = s^{i}(1-\eta)/2 + s^{j}(1+\eta)/2; \quad (20)$$
$$x = x^{i}(1-\eta)/2 + x^{j}(1+\eta)/2.$$

Nodal unknown variables of the finite element for j loading steps are represented by components of the displacement vector and their derivatives in the local coordinate system

$$\left\{U_{\mathrm{y}}\right\}^{\mathrm{T}} = \{\{\upsilon^{\gamma}\}^{\mathrm{T}}\{\upsilon\}^{\mathrm{T}}\}, \quad (21)$$

where $\{\upsilon^{\gamma}\}^{\mathrm{T}} = \left\{\upsilon^{1i}\upsilon^{1j}\upsilon_{,\eta}^{1i}\,\upsilon_{,\eta}^{1j}\right\}$; $\{\upsilon\}^{\mathrm{T}} = \left\{\upsilon^{i}\upsilon^{j}\upsilon_{,\eta}^{i}\,\upsilon_{,\eta}^{j}\right\}$.

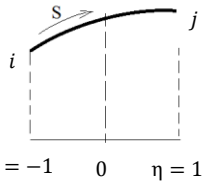

Fig. 1. Discretization element at the loading stage

At step (j+1), nodal variable parameters are determined as follows

$$\{\Delta U\}^{\mathrm{T}} = \{\{\Delta\upsilon^{\gamma}\}^{\mathrm{T}}\{\Delta\upsilon\}^{\mathrm{T}}\}, \quad (22)$$

where$\{\Delta\upsilon^{\gamma}\}^{\mathrm{T}} = \left\{\Delta\upsilon^{1i}\Delta\upsilon^{1j}\Delta\upsilon_{,\eta}^{1i}\,\Delta\upsilon_{,\eta}^{1j}\right\}$;
$\{\Delta\upsilon\}^{\mathrm{T}} = \left\{\Delta\upsilon^{i}\Delta\upsilon^{j}\Delta\upsilon_{,\eta}^{i}\,\Delta\upsilon_{,\eta}^{j}\right\}$.

Derivatives in the local coordinate system are determined through derivatives in the global coordinate system as follows

$$\frac{\partial q}{\partial\eta} = \frac{\partial q}{\partial s}\frac{\partial s}{\partial\eta}; \quad \frac{\partial^2\upsilon}{\partial\eta^2} = \frac{\partial^2\upsilon}{\partial s^2}\left(\frac{\partial s}{\partial\eta}\right)^2, \quad (23)$$

where q a meridional υ^1 or normal υ component of the displacement vector.

The displacements of the internal FE point at the (j + 1) loading step are expressed by the relations

$$\Delta\upsilon^{1} = \{\varphi\}^{\mathrm{T}}\{\Delta\upsilon^{1}\}, \Delta\upsilon = \{\varphi\}^{\mathrm{T}}\{\Delta\upsilon\}. \quad (24)$$

Forjloading steps

$$\upsilon^{1} = \{\varphi\}^{\mathrm{T}}\{\upsilon^{1}\}, \upsilon = \{\varphi\}^{\mathrm{T}}\{\upsilon\}. \quad (25)$$

The matrix $\{\varphi\}^{\mathrm{T}}$included in (24), (25) is determined through the чрезHermite polynomials of the third degree

$$\{\varphi\}^{\mathrm{T}}=\{h_1h_2h_3h_4\}. \quad (26)$$

Thus, expressions (24) and (25) can be written in matrix form

$$\{\Delta U\} = [\mathrm{A}]\left\{\Delta U_{\mathrm{y}}\right\}; \{U\} = [\mathrm{A}]\left\{U_{\mathrm{y}}\right\}. \quad (27)$$

By differentiating (24) and (25), taking into account (23), the derivatives of the components of the displacement vector in the global coordinate system are determined as follows:

$$q_{,\mathrm{s}} = \left\{\varphi_{,\eta}\right\}^{T}\frac{\partial\eta}{\partial S}\{q\};$$
$$\upsilon_{,ss} = \left\{\varphi_{,\eta\eta}^{2}\right\}^{T}\left(\frac{\partial\eta}{\partial S}\right)^2\{\upsilon\}, \quad (28)$$

where $\frac{\partial\eta}{\partial S} = \frac{2}{(s^{i}-sj)}$.

2.3 Relations between strains and stresses at the loading step

To take into account the physical nonlinearity of the material used, the relations of the deformation theory of plasticity are used [14]

$$\varepsilon_{ij}\text{-}\delta_{ij}\varepsilon_0=\frac{3}{2}\frac{\varepsilon_i}{\sigma_i}\left(\sigma_{ij}-\delta_{ij}\sigma_0\right);(i,j=1,2,3), \quad (29)$$

where $\varepsilon_0=\frac{\varepsilon_{11}^{\zeta}+\varepsilon_{22}^{\zeta}+\varepsilon_{33}^{\zeta}}{3}$ – average linear strain;
$\sigma_0=\frac{\sigma_{11}+\sigma_{22}+\sigma_{33}}{3}$ – average linear stress;
ε_i – strain intensity; σ_i – stress intensity; δ_{ij} – Kronecker symbol.

For axisymmetric deformation, relations (29) can be written as

$$\begin{aligned}\varepsilon_{11}^{\zeta}&=(\sigma_{11}-\sigma_0)\frac{3\varepsilon_i}{2\sigma_i}+\mathrm{K}\sigma_0;\\ \varepsilon_{22}^{\zeta}&=(\sigma_{22}-\sigma_0)\frac{3\varepsilon_i}{2\sigma_i}+\mathrm{K}\sigma_0;\\ \varepsilon_{33}^{\zeta}&=(-\sigma_0)\frac{3\varepsilon_i}{2\sigma_i}+\mathrm{K}\sigma_0,\end{aligned} \quad (30)$$

where $\sigma_0=\frac{\sigma_{11}+\sigma_{22}}{3}$; $\mathrm{K}=\frac{E}{1-2\mu}$; μ – Poisson's ratio.

Coefficient K in (30) was determined in [14] using the assumption that, as a result of plastic deformations, the volume does not change.

This coefficient was determined from a simple tensile experiment based on the relations

$$\begin{aligned}\sigma_0=\frac{\sigma_{11}+\sigma_{22}+\sigma_{33}}{3}=\frac{\sigma}{3};\ \varepsilon_0=\frac{\varepsilon_{11}^{\zeta}+\varepsilon_{22}^{\zeta}+\varepsilon_{33}^{\zeta}}{3}=\frac{1-2\mu}{3}\varepsilon;\\ \sigma_i=\sigma;\ \varepsilon_i=\varepsilon\frac{2}{3}(1+\mu),\end{aligned} \quad (31)$$

As a result we have

$$\mathrm{K}_1=\frac{2(1+\mu)}{3(1-2\mu)}\frac{\sigma_i}{\varepsilon_i}. \quad (32)$$

As can be seen, coefficient K_1 is a function of the parameters of the curve of the material deformation diagram.

Relations for strain increments through stress increments are obtained by differentiating (30)

$$\begin{aligned}\Delta\varepsilon_{\alpha\alpha}^{\zeta}=\frac{\partial\varepsilon_{11}^{\zeta}}{\partial\sigma_{\alpha\alpha}}\Delta\sigma_{\alpha\alpha}+\frac{\partial\varepsilon_{22}^{\zeta}}{\partial\sigma_{\alpha\alpha}}\Delta\sigma_{\alpha\alpha}+\\ +\frac{\partial}{\partial\sigma_{\alpha\alpha}}(\mathrm{K}_1\sigma_0)\Delta\sigma_{\alpha\alpha}.\end{aligned} \quad (33)$$

Based on relation (33), a matrix expression is formed

$$\left\{\Delta\varepsilon_{\alpha\beta}^{\zeta}\right\}=[D]\left\{\Delta\sigma_{\alpha\beta}\right\}, \quad (34)$$

where $[D]$ – the matrix of the stress-strain state of the material.

2.4 The stiffness matrix at the loading stage

When deriving the FE stiffness matrix at the (j + 1) **l**oading stage of loading, we used the functional F written on the basis of the equality of the work of external and internal forces at a possible displacement

$$\begin{aligned}\mathrm{F}=\int_{\mathrm{V}}\left\{\Delta\varepsilon_{\alpha\beta}^{\zeta}\right\}^{\mathrm{T}}\left(\left\{\sigma_{\alpha\beta}\right\}+\left\{\Delta\sigma_{\alpha\beta}\right\}\right)\mathrm{dV}\\ -\int_{\mathrm{F}}\{\Delta U\}^{\mathrm{T}}(\{\mathrm{P}\}+\{\Delta\mathrm{P}\})\,\mathrm{dF},\end{aligned} \quad (35)$$

where $\left\{\Delta\varepsilon_{\alpha\beta}^{\zeta}\right\}^{\mathrm{T}}=\left\{\Delta\varepsilon_{11}^{\zeta}\Delta\varepsilon_{22}^{\zeta}\right\}$ – the matrix-row of strain increments at the loading stage;
$\left\{\sigma_{\alpha\beta}\right\}^{\mathrm{T}}=\{\sigma_{11}\sigma_{22}\}$, $\left\{\Delta\sigma_{\alpha\beta}\right\}^{\mathrm{T}}=\{\Delta\sigma_{11}\Delta\sigma_{22}\}$ – matrix-rows of stresses and their increments in an arbitrary layer of the shell of revolution;
$\{\Delta U\}^{\mathrm{T}}=\{\Delta\upsilon^1\Delta\upsilon\}$ – the matrix-row of increments of the components of the displacement vector at the (j + 1)-th loading stage;
$\{\mathrm{P}\}^{\mathrm{T}}=\{\mathrm{P}_{11}\mathrm{P}_{22}\}$, $\{\Delta\mathrm{P}\}^{\mathrm{T}}=\{\Delta\mathrm{P}_{11}\Delta\mathrm{P}_{22}\}$ – surface load and its increments at the (j + 1) -th loading stage.

The strain increment matrix can be represented as

$$\left\{\Delta\varepsilon_{\alpha\beta}^{\zeta}\right\}=[\Gamma][\mathrm{B}]\left\{\Delta U_{\mathrm{y}}^{l}\right\}. \quad (36)$$

The increments of stresses in an arbitrary layer of the shell of revolution are as follows

$$\left\{\Delta\sigma_{\alpha\beta}\right\}=\left[C_{pl}\right]\left\{\Delta\varepsilon_{\alpha\beta}^{\xi}\right\}, \quad (37)$$

where $\left[C_{pl}\right]$ is determined from з (34).

The increments of the components of the displacement vector at the (j + 1) th loading step are determined according to (27).

When substituting expressions (27), (36) and (37) into functional (35) and performing its minimization with respect to nodal unknowns, the expression

$$[\mathrm{M}]\left\{\Delta U_{\mathrm{y}}^{g}\right\}=\{F\}+\{f\}, \quad (38)$$

where $[\mathrm{M}]=\int_V\{\mathrm{B}\}^{\mathrm{T}}\{\Gamma\}^{\mathrm{T}}\left[C_{\mathrm{pl}}\right][\Gamma][\mathrm{B}]\,\mathrm{d}V$ – the stiffness matrix of the final element of the shell of revolution at the loading stage; $[F]^{\mathrm{T}}=\int_F\{\mathrm{A}\}^{\mathrm{T}}\{\Delta\mathrm{P}\}\mathrm{d}F$ – the vector of external loads at the loading stage;
$[\mathrm{f}]^{\mathrm{T}}=\int_F\{A\}^{\mathrm{T}}\{P\}dF-\int_V\{\mathrm{B}\}^{\mathrm{T}}\{\Gamma\}^{\mathrm{T}}\{\sigma\}dV$ – Newton-Raphson correction.

3 Results

As an example, the problem was solved to determine the stress-strain state of a complex-jointed shell structure shown in Figure 2.

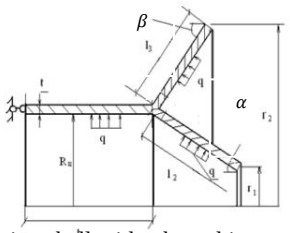

Fig. 2. Revolution shell with a branching meridian

The following data were used: internal pressure q=0.7 MPa; Poisson's ratio$\mu=0.32$; elastic modulus $E=7\cdot10^5$ MPa; radius of a cylindrical shell R_c=0.9 m; cylinder length L_c=0.8 m; shell thickness t=0.01m; cone lengths L_{lk}=1.1 m. and L_{uc}=0.2 m; angle $\alpha=45^0$, angle $\beta=30^0$. The left edge of the structure has a hinged bearing (Fig. 2). A sufficient convergence of the computational process took place when each branch of the structure was divided into 12 FEs.

In the software implementation of the step procedure, for simplicity of calculations, a strain diagram with linear hardening was used

$$\sigma_i = \sigma_0 + p(\varepsilon_i - \varepsilon_T), \quad (39)$$

where $\sigma_0 = 200$ MPa; $\varepsilon_T = 0.0023496$ m; p = 18087.03 MPa.

When articulating the three shells of revolution at the branching point of the meridian, the correct kinematic and static conjugation conditions were used: the invariance of the displacement vectors, as well as the equality of the angles of rotation of the normals to the median surfaces before and after deformation [15].

The calculation was performed in two versions. In the first version (Table 1), when deriving the plasticity matrix at the loading step, we used coefficient K, which determines the relationship between the average linear stress $\sigma_0$and the average linear strain ε_0, without taking into account compressibility at elastic plastic deformations. In the second version (Table 2), coefficient K_1 determined in (32) was applied. The number of loading steps in the first and second versions varied from 30 to 100.

Table 1. Calculation option 1.

Stress, MPa		Number of loading steps , n_s		
		30	70	100
Reference section, x = 0.0 m	σ_m^u	23.25	23.41	23.45
	σ_m^{av}	23.23	23.40	23.52
	σ_m^l	23.22	23.39	23.43
Meridian branching unit, x = 0.8 m	σ_{1m}^u	–286.51	–419.29	–543.72
	σ_{1m}^{av}	–263.65	–405.67	–532.21
	σ_{1m}^l	–258.47	–392.01	–520.7
	σ_{2m}^u	–300.88	–614.78	–998.38
	σ_{2m}^{av}	–17.74	–494.91	–874.67
	σ_{2m}^l	279.46	–374.76	–750.95

Table 2. Calculation option 2.

Stress, MPa		Number of loading steps , n_s		
		30	70	100
References ection, x = 0.0 m	σ_m^u	22.27	23.03	23.18
	σ_m^{av}	22.67	23.02	23.17
	σ_m^l	22.56	23.00	23.16
Meridian branching unit, x = 0.8 m	σ_{1m}^u	117.88	97.70	108.51
	σ_{1m}^{av}	48.86	56.95	58.64
	σ_{1m}^l	–72.87	–112.71	–133.26
	σ_{2m}^u	279.19	282.78	270.8
	σ_{2m}^{av}	–80.10	–97.01	–102.45
	σ_{2m}^l	–306.96	–322.6	–338.52

The results of finite element solutions are presented in Tables 1 and 2. They show the numerical values of the meridional stresses at the points of the calculated structure: in the reference section (x = 0.0) and in the branch node of the meridian (x = 0.8 m). Values of the parameters are given for internal (σ_m^u) and external (σ_m^l) fibers, and for the points of the middle surface of the revolution shell σ_m^{av}. The branch node represents stresses of the elements of adjacent shells: σ_{1m}^u ,σ_{1m}^{av},σ_{1m}^l – for the lower cone and σ_{2m}^u ,σ_{2m}^{av},σ_{2m}^l – for the upper one.

4 Discussion

The results were verified according to the convergence of the computing process and the comparison of the values of the controlled parameters of the stress-strain state with the values calculated using well-known formulas obtained from the equilibrium equation.

The analysis showed that in the reference section of the structure, the convergence of the computational process is satisfactory for both calculation options.

At the branching node of the meridian, that is, in the zone of stress concentration, the results of finite-element solutions differ from each other in the first and second versions of the calculation. In the first version, a significant increase in the values of the meridional stresses in the branching node is observed, which is not reliable with the value of the specified load. With an increase in the number of loading steps in the first embodiment, the controlled parameters of the stress-strain state increase in their absolute values so that the convergence of the computational process is not observed. For the lower cone with a number of steps equal to 100, an increase in the meridional stress indices by 50% is observed in comparison with the values when the number of steps n = 70.

In the second version, there are no sharp increase in stresses in the branching node. In addition, in the second version, according to the calculation scheme (Fig. 2), the lower cone works in tension, and the upper one works in compression. For the first version of the calculation, this correspondence is not observed. With an increase in the number of loading steps in the second version, the values of the meridional stresses at the branching node of the meridian change insignificantly, which indicates the satisfactory convergence of the computational process.

In the reference section, the value of the meridional stress at the points of the middle surface can be calculated based on the equilibrium condition (Fig. 2)

$$\sigma_{calc}^m = \frac{q\pi}{t}\left(\frac{\mathrm{R}_c^2 - \mathrm{r}_1^2}{2\pi \mathrm{R}_\mathrm{c}} - \frac{\mathrm{r}_2^2 - \mathrm{R}_c^2}{2\pi \mathrm{R}_c}\right). \quad (40)$$

Substituting the initial data in (39), we have

$$\sigma_{calc}^m = \frac{7}{1}\left(\frac{(90)^2 - (12.2)^2}{2\cdot 90} - \frac{(100)^2 - (90)^2}{2\cdot 90}\right) = 23.11\ MPa \quad (41)$$

As can be seen from the Tables, both options allow us to obtain the exact solution of the reference section. The calculation error does not exceed 1%.

5 Conclusion

It can be concluded that the algorithm for the formation of a plasticity matrix at the loading stage, when calculating complex shell structures, allows us to obtain finite element solutions acceptable for the design engineering practice. They can be recommended for using in design systems when analyzing the stress-strain state of agricultural facilities. The relationship between the average linear stress σ_0 and the average linear strain ε_0 during the plasticity matrix formation can be implemented in the form (32).

Acknowledgments

The study was financially supported by the Russian Fundamental Research Fund and Volgograd Region Administration No. 19-41-340002 r_a.

References

1. R.A. Kayumov, *Postbuckling behavior of compressed rods in an elastic medium*, Mechanics of Solids, **52(5)**, 575–580 (2017)
2. I.B. Badriev, V.N. Paimushin, *Refined models of contact interaction of a thin plate with postioned on both sides deformable foundations*, Lobachevskii J. of Mathem., **38(5)**, 779–793 (2017)
3. V.A. Kozlov, *Stress-strain of elements of bridge structures with varying thickness of walls along the length*, Russ. J. of Build. Construct. and Architect., **1(37)**, 67–80 (2018)
4. V.A. Ignatiev, *Calculation of plane frames with large displacement of nodes by the finite element method in the form of the classical mixed method*, J. of Construct. and reconstruct., **2(58)**, 12–19 (2015)
5. K.P. Pyatikrestovsky, B.S. Sokolov, *Nonlinear analysis of statically ideterminate wooden structures and optimization of cross section dimensions of dome ribs*, Int. J. for Computat. Civil and Structur. Engineer., **14(4)**, 130–139 (2018)
6. V.V. Karpov, O.V. Ignatev, A.A. Semenov, *The stress-strain state of ribbed shell structures*, Magazine of Civil Engineer., **74(6)**, 147–160 (2017)
7. K.Yu. Bate, *Numerical methods* (Physic. and mathemat. Lit, Moscow, 2010)
8. V.P. Agapov, R.O. Golovanov, K.R. Aidemirov, *Calculation of load bearing capacity of prestressed reinforsced concrete trusses by the finite element method*, IOP Conf. Ser. Earth and Environmental Sci., **90**, 01 2018 (2017)
9. V.P. Agapov, R.O. Golovanov, *Comparative analysis of the simplest finite elements of plates inbending*, Advances in Intelig. Syst. and Comput., **692**, 1009–1016 (2018)
10. Y.V. Klochkov, A.P. Nikolaev, A.Sh. Dzhabrailov, *Finite element analysis of axisymmetrically loaded shells of rotation with branching meridian under elastic-plastic deformation*, J. of Struct. Mechan. of Engineer. Constr. and Buildings, **3**, 50–56 (2013)
11. E.A. Souza Neto, D. Peric, D.R.J. Owen, *Computational Methods for Plasticity, Theory and Applications*, Chichester: Wiley Mechan. and Engineer., **268**, 704–734 (2008)
12. C. Miehe, F. Welschinger, F. Aldakheel, Variational gradient plasticity at finite strains *Computer Methods in Applied Mechanics and Engineering* (2014)
13. L.I. Sedov, *Continuum Mechanics*, vol. 1 (Nauka, Moscow, 1976)
14. M.M. Malinin, *Applied Theory of Plasticity and Creep* (Engineering, Moscow, 1975)
15. A.Sh. Dzhabrailov, Yu.V. Klochkov, A.P. Nikolaev, *The Finite Elements Analysis of Shells of Revolution with a Branching Meridian*, J. Russ. Aeronaut., **52(1)**, 22–29 (2009)